SECOND EUROPEAN CONFERENCE ON EARTHQUAKE ENGINEERING AND SEISMOLOGY, ISTANBUL AUG. 25-29, 2014

SEISMIC FRAGILITY CURVES FOR REINFORCED CONCRETE BUILDINGS AND BRIDGES IN THESSALONIKI

Georgios TSIONIS[1] and Michael N. FARDIS[2]

ABSTRACT

Fragility curves are developed for the reinforced concrete buildings and bridges in the city of Thessaloniki, for use in the systemic seismic vulnerability and risk analysis of the urban area. The methodology is based on nonlinear analysis of simplified models and accounts for uncertainties in the demand and capacity quantities due to modelling and the variability of materials, geometry as well as of the seismic action. The fragility curves show that buildings may suffer minor damage for the design earthquake and that there is a safety margin before severe damage appears. The probability of damage on bridges is low for the design earthquake, but some may need to be closed to traffic. The results verify the favourable effect of modern seismic codes in substantially reducing the expected damage of structures. It is also demonstrated that the fragility curves of bridges vary significantly with their geometry, even for bridges having the same structural configuration.

INTRODUCTION

The European collaborative research project SYNER-G (Pitilakis et al., 2014) focused on systemic seismic vulnerability and risk analysis of buildings, lifelines and infrastructures. The methodology and tools developed within the project were applied to a number of case studies. The work presented in this paper is a contribution to the validation study in the city of Thessaloniki, the second largest in Greece. It is located in a moderate-seismicity region and hosts important administrative, economic, industrial and academic activities.

As regards reinforced concrete (RC) buildings, fragility curves are developed for prototype buildings that are representative of the typologies in the building stock. Both flexural and shear failure are considered; the latter was disregarded in past fragility studies for the buildings in Thessaloniki. An additional contribution is the development of fragility curves for wall-frame (dual) buildings designed with a modern seismic code, which were not available for the study area.

The existing studies on the seismic fragility of RC bridges in Europe focus mainly on modern structures and ignore the possibility of shear failure of the piers. Besides, bridges belonging to the same structural class may have different fragilities because of their specific geometric characteristics. For the above reasons, new fragility curves are produced for individual bridges in the Thessaloniki study area, based on the actual properties of each structure.

The methodology used for the fragility analysis employs nonlinear analysis of simplified models of the examined buildings and bridges, following the rules and seismic assessment procedure in Part 3 of Eurocode 8 (CEN, 2005c). It accounts for model uncertainties, the variability of materials and geometry and that of the seismic action for given peak ground acceleration (PGA).

[1] PhD, European Commission, Joint Research Centre, Ispra, Italy, georgios.tsionis@jrc.ec.europa.eu (formerly at University of Patras)
[2] Professor, University of Patras, Patras, Greece, fardis@upatras.gr

BUILDING AND BRIDGE TYPOLOGIES

The study area, described in detail by Pitilakis et al. (2014), comprises mainly the municipality of Thessaloniki with a population of 376.589 and a predominantly residential land use. The inventory includes 27.738 buildings, 92 % of which are RC buildings and the remaining are masonry buildings. The majority of RC buildings were constructed before 1980 and therefore were designed with a “low-level” seismic code. The most common structural type is the wall-frame (dual) system.

For the purpose of this work, the RC buildings are classified on the basis of the structural system (infilled frames, frames with open ground storey and dual buildings), level of seismic design (“low”, “medium” and “high”) and height (low-, mid- and high-rise buildings). Fragility curves are developed for prototype regular buildings, whose plans are shown in Figure 1. The geometry and reinforcement of the prototype buildings designed with the “low- and “medium-level” seismic codes originate from a set of buildings designed by Kappos et al. (2003) according to the Greek seismic codes of 1959 (“low-level”) and 1984 (“medium-level”). The “high-level” code buildings in the inventory are dual systems. In the present application, they are designed according to Eurocode 8 (CEN 2004) for Medium Ductility Class and PGA 0.16g, following the procedure described by Fardis et al. (2012). Low-, mid- and high-rise buildings have respectively two, four and nine storeys. Permanent loads, including the dead weight of the structure, finishings, partitions and façades, amount to 7 kN/m^2. The nominal value of occupancy loads is 2 kN/m^2.

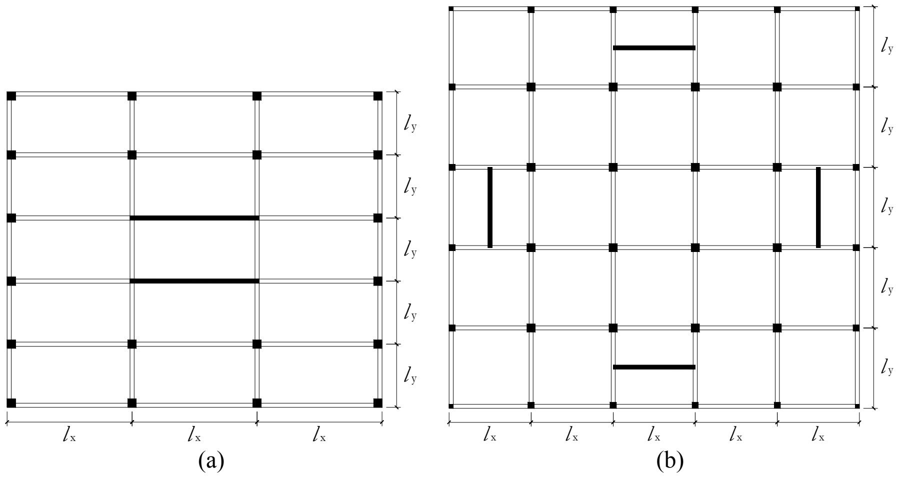

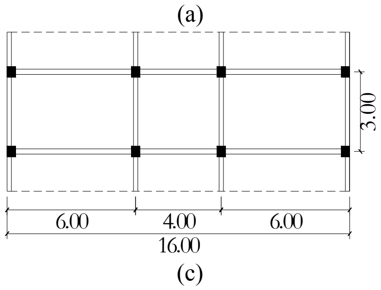

	Low-, medium-level code		High-level code	
	l_x (m)	l_y (m)	l_x (m)	l_y (m)
Low-, mid-rise	4.0	4.5	4.0	4.0
High-rise	6.0	3.0	6.0	6.0

Figure 1. Plan of prototype buildings: dual buildings designed with “low- and “medium-level” code (a), dual buildings designed with “high-level” code (b) and frame buildings (c)

The road network examined in the application includes the main urban roads, the internal and external ring roads and the principal connections with the highway network. There are 60 bridges in the study area, the majority of which are located on the ring roads and connections. Fragility curves are developed for 22 bridges for which construction drawings with sufficient details were available. The remaining bridges are associated to the most appropriate type among those 22, on the basis of their structural characteristics. Table 1 lists their main features, i.e. deck continuity (continuous deck or movement joints over one or more supports), deck-pier connection (monolithic, through bearings, or combination), transverse translation at ends (free or restrained), construction year, pier type (single-column, wall, multi-column), maximum pier height and span lengths. Geometry, reinforcement and material properties are taken from the design drawings. Deck types include solid slabs, slabs with voids, box girders and precast girders with concrete topping. Concrete classes range from C15/12 to C35/40. The steel used in the piers is S500 and in some cases S400 for the horizontal reinforcement.

Table 1. Classification of RC bridges in Thessaloniki

Structural system	Type	Transverse translation at ends	Construction year	Pier type	Max. pier height (m)	Span lengths (m)
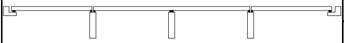 Bearings, deck with expansion joints	B01	free	1984	multi-column	11.6	15+25×30+15
	B02	free	1986	multi-column	8.0	37+5×35+34
	B05	free	1985	multi-column	3.7	4×31
	B09	free	1990	single-column	5.7	2x27
	B22	free	1991	multi-column	8.4	21+25
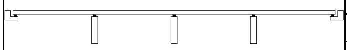 Bearings, continuous deck	B03	free	1991	wall	7.5	33+33+10
	B06	free	2002	multi-column	6.5	18+37+40+17
	B17	free	1992	wall	8.0	20+37+20
	B18	free	1992	wall	8.0	3×18
	B20	free	1985	wall	20.0	3×40
	B21	free	1985	wall	22.0	3×40
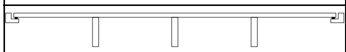 Monolithic connection, continuous deck	B04	restrained	2000	multi-column	7.1	34+22+44+34
	B19	free	2004	wall	15.2	19+31+19
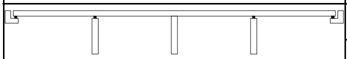 Monolithic connection at some piers, bearings at the rest, continuous deck	B07	restrained	2003	single-column	6.2	28+3×35+28
	B08	restrained	2003	single-column	5.3	24+31+32+35+28
	B15	restrained	2002	single-column	11.4	18+26+17+31+15+22+19
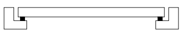 Single-span bridges on bearings	B10	free	1976	-	-	28
	B11	free	1985	-	-	20
	B12	free	1990	-	-	32
	B13	free	1985	-	-	22
	B14	free	1987	-	-	40
	B16	free	1994	-	-	21

In half of the bridges in the study area the deck (continuous or with intermediate expansion joints) is supported on bearings. The second most common type (27 % of the total) is the single-span bridge on bearings. Bridges with monolithic deck-pier connection make up 13 % of the population. The remaining 10 % are bridges with the deck monolithically connected to the central piers and supported by bearings on the other supports. Bridges constructed after 1993 are considered to have been designed with a "high-level" seismic code and amount to 37 % of the total number of bridges in the study area. Those designed with a "medium-level" code, constructed between 1986 and 1993, account for 30 % of the inventory. The remaining bridges (33 % of the total) were constructed before 1986 and were designed with a "low-level" code.

DAMAGE STATES, DAMAGE MEASURES AND INTENSITY MEASURE

Fragility curves are constructed for two damage states: yielding and ultimate. PGA is used as intensity measure. The PGA of the excitation has been preferred over more efficient and informative alternatives (such as the spectral displacement at the fundamental period for ductile failure modes, or the spectral acceleration for brittle ones) for consistency with the use of design PGA as the main seismic design parameter.

The damage measure used for member yielding and ultimate condition in flexure is the chord rotation at the member ends. For the member ultimate condition in shear, it is the shear force outside the plastic hinge or inside it, considered then alongside the value of the rotation ductility factor at the end of the member. In bridges where the deck is supported on bearings, the damage measures for the ultimate state of bearings are the relative displacement between the deck and the top of the support, checked against the eccentricity of vertical load that leads to rollover, and the shear deformation of the bearings.

Fragility results are obtained separately for each type of member and storey in buildings. If perfect correlation is assumed between members of the same type (i.e., beams or columns) in a storey, the fragility curve of a single interior member of this type may be taken to apply to the entire ensemble of such members in the storey. For each value of PGA, the most critical element and failure mode in all storeys determine the fragility curves for the whole building.

Fragility curves are constructed for each pier or bearing for the seismic action separately in the transverse and the longitudinal direction of the bridge. The fragility curve of a component at the ultimate damage state is taken as the worse of its possible conditions: flexural or shear failure for piers and rollover or shear deformation for bearings. The most critical element, failure mode and direction at each value of PGA determine the fragility curves for the whole bridge. In bridges with expansion joints in the deck, the parts with continuous deck are treated as independent sub-structures and the most critical components are considered for the yielding and ultimate damage states of the bridge system.

FRAGILITY ANALYSIS

A methodology which avoids time-consuming calculations is followed. It uses as input the basic geometry and reinforcement details of the structure and produces the fragility curves with minimal computational demand. Fragility curves are established point-by-point. The values of damage measure demands of interest are obtained at each PGA level from the deterministic seismic analysis outlined in the following sections and are considered as conditional-on-PGA median values of these demands.

The mechanical interaction of the damage states between different elements is considered only in a mean sense. As the analysis is deterministic (see following sections) and based on mean properties, the demand on a member or on a failure mode is computed assuming that yielding of another member has been reached only if it has taken place with a conditional-on-PGA probability of at least 50 %. The deterministic analysis does not take into account the mechanical effect on other members of the drop in lateral force resistance by at least 20 %, which is considered to accompany attainment of a member's ultimate damage state.

The median values of the damage measure capacities for the two damage states of component yielding and ultimate are determined according to Part 3 of Eurocode 8 (CEN, 2005c) for RC members in buildings and bridges and EN 1337 (CEN 2005a) for bearings. The variances of both demand and capacity measures are estimated from the values of their coefficients of variation.

The value of a component's fragility for each one of the damage states considered is obtained at each PGA level at which the deterministic seismic analysis is carried out as the probability that the random variable of demand (for given PGA) exceeds the random variable of capacity. The first two moments of these random variables are derived from those of the pertinent basic random variables. If the random variable of demand or capacity is related to the pertinent basic random variable through a multiplicative function (as in the case of the flexural damage states), lognormal distributions of the individual random variables are assumed. If this function is additive (as in the dependence of the shear resistance of a plastic hinge on the rotation ductility demand at the member end), normal distributions are used instead. Then, the fragility curves at the system level (building or bridge) do not always follow the lognormal distribution. For practical reasons, though, a lognormal cumulative probability function is fitted to the fragility curves of the system and its mean value, μ, and standard deviation, β, are computed for use in the application.

ANALYSIS OF BUILDINGS

Deterministic estimates of damage measures are obtained for each value of the excitation PGA via a static analysis under a unidirectional set of lateral forces with an inverted triangular pattern, following the modelling assumptions, approach and methods provided in Part 3 of Eurocode 8 (CEN, 2005c) for the seismic performance assessment of existing regular buildings. The seismic action is defined by the Type 1 spectrum of Eurocode 8 for ground type C (firm soil). The analyses use mean material properties and the secant-to-yield-point rigidity.

Vertical elements are taken as fixed at ground level. Beam-column joints and floor diaphragms are taken as rigid. P-Δ effects due to the seismic action are included in the analysis. Bending moments due to gravity loads are considered negligible.

Generic members considered in the models are limited for simplicity to the interior columns and beams in wall-frame or frame systems and the walls of wall-frame systems. The effect of perimeter columns and beams on the response of interior members may be ignored, if perimeter members have about one-half the rigidity of interior ones at the same storey. Then, all beam ends in a storey of a frame have the same elastic seismic moments and inelastic chord rotation demands. The same applies to all interior columns of the frame, with exterior columns developing one-half the elastic seismic moments of same-storey interior ones, but the same inelastic seismic chord rotation demands. Besides, the axial force variation due to the seismic action is neglected in interior columns.

Once plastic hinges start forming in the structure, shear forces in beams and columns are calculated from the plastic mechanism and the yield moments of the sections that have already yielded. As nonlinear dynamic effects are ignored in the analysis, once a plastic hinge forms at a wall base, the shears up the wall are amplified for inelastic higher mode effects according to the proposal of Keintzel (1990), adopted also by Eurocode 8 (CEN, 2004) for Ductility Class High walls. The fragility curves obtained from this analysis approach for column and beams were found to be in very good agreement to those from nonlinear response-history analysis or full-fledged pushover analysis of a complete 3D model in three pure frame and in 16 wall-frame buildings with five or eight storeys, designed to Eurocode 8 for Ductility Class Medium or High (Antoniou et al., 2014). However, the nonlinear response-history analyses in (Antoniou et al., 2014), have shown that this procedure overestimates the actual amplification of wall shear forces. Then, the fragility of walls for shear failure was taken as the average of the fragilities computed with the post-elastic amplification as above and with no amplification, as suggested by the results in (Antoniou et al., 2014).

ANALYSIS OF BRIDGES

Displacement and deformation demands for bridge components are estimated from analysis with the 5 %-damped elastic spectrum and the “equal displacement rule”. The permanent loads comprise the self-weight together with 20 kN/m for the sidewalks and 2 kN/m^2 for deck surfacing. Traffic load models from Eurocode 1 (CEN, 2003) are adopted. Seismic analysis is performed for the Type 1 spectrum of Eurocode 8, modified according to Pitilakis et al. (2012), and the ground type at the location of each bridge.

Elastic analysis is performed using the secant-to-yield-point stiffness of the piers computed with mean material strengths. If the pier supports the deck via bearings, the effective stiffness of piers for use in the seismic analysis is taken equal to the stiffness of the uncracked gross section. If the pier is monolithically connected to the deck, its secant stiffness at the yield point is used, as calculated from the design ultimate moment and the section’s yield curvature per Part 2 of Eurocode 8 (CEN 2005b). The piers are taken as fixed at their base.

The “rigid deck model” of Eurocode 8 (CEN 2005b) is used in the longitudinal direction of all the bridges and in the transverse direction of those with free transverse translation at the abutments. The model consists of a single-degree-of-freedom system of the deck with the total mass of the deck added to the masses in the upper half of all piers which are rigidly connected to the deck, and the total stiffness of the individual supports. The composite pier-bearing stiffness is used for the piers that support the deck via bearings and the deck displacement is attributed to the pier and the bearing in proportion to their flexibilities. In the transverse direction of bridges with the deck monolithically connected to single-column piers, the rotational degree-of-freedom at the pier top is slaved to the horizontal translation there, so as to consider the effect of the rotational mass moment of inertia of the deck about its axis.

In the transverse direction of bridges with constrained transverse translation at the abutments, modal response spectrum analysis is performed. The mass of the deck is distributed along its length and half of the mass of each pier is lumped at its top. In bridges with up to three intermediate supports, the piers are considered discretely. If the piers are more than three, their transverse stiffness is smeared along the deck, which is then considered as a beam on a continuous elastic lateral support. The modal properties of symmetric bridges are calculated via closed-form solutions (Fardis and Tsionis 2013).

UNCERTAINTIES

The dispersions of demand and capacity measures of building components are calculated from the coefficients of variation (CoV) listed in Table 2. The coefficients of variation for the chord rotation demands are based on extensive comparisons of inelastic chord rotation demands in height-wise regular multi-storey buildings to their elastic estimates (Panagiotakos and Fardis, 1999; Kosmopoulos and Fardis, 2007), whereas the values for the shear force demands are based on parametric studies. Those of the capacities reflect the uncertainty in the models used for the estimation of the mean values and the scatter of material and geometric properties about their best estimates (Biskinis and Fardis, 2010a; 2010b; Biskinis et al., 2004).

Table 2. Coefficients of variation for demand and capacity measures of building components

Demand	CoV	Capacity	CoV
Beam chord rotation demand, for given spectral value at the fundamental period	0.25	Beam or column chord rotation at yielding	0.33
Column chord rotation demand, for given spectral value at the fundamental period	0.20	Beam or column ultimate chord rotation	0.38
Wall chord rotation demand, for given spectral value at the fundamental period	0.25	Shear resistance in diagonal tension (inside or outside plastic hinge)	0.15
Beam shear force demand, for given spectral value at the fundamental period	0.10	Wall chord rotation at yielding of the base	0.40
Column shear force demand, for given spectral value at the fundamental period	0.15	Wall ultimate chord rotation at the base	0.32
Wall shear force demand, for given spectral value at the fundamental period	0.20	Wall shear resistance in diagonal compression	0.175
Spectral value for given PGA and fundamental period	0.25		

Table 3. Coefficients of variation for demand and capacity measures of bridge components

Demand	CoV	Capacity	CoV
Spectral value for given PGA and fundamental period	0.25	Shear resistance in diagonal tension, circular pier	0.16
Shear force demand for given spectral value at fundamental period	0.15	Shear resistance in diagonal tension, rectangular or hollow pier	0.14
Displacement demand for given spectral value at fundamental period	0.20	Shear resistance in web compression, rectangular or hollow pier	0.18
Daily temperature	0.67	Yield chord rotation, circular pier	0.32
Creep and shrinkage strains	0.60	Yield chord rotation, rectangular or hollow pier	0.29
		Ultimate chord rotation, circular pier	0.30
		Ultimate chord rotation, rectangular pier	0.36
		Ultimate chord rotation, hollow pier	0.29
		Deformation capacity of bearings	0.30

Table 3 collects the coefficients of variation for demand and capacity measures of bridge elements. The values for the pier deformation demands for given excitation spectrum are based on the numerical analyses reported by Bardakis and Fardis (2011). Those for creep and shrinkage are based on the scatter associated with the models used and the natural dispersion of the variables they use. The coefficients of variation of the pier capacities have been quantified from experimental data (Biskinis and Fardis 2010a, 2010b, 2013; Biskinis et al. 2004). Those for the bearings are established from the literature, alongside cyclic tests on elastomeric and lead rubber bearings tested at the Structures Lab of the University of Patras. The coefficient of variation of daily temperature derives from the presumed standard deviation and yearly mean, 10 and 15 ^{o}C respectively.

Spectral values of individual motions at the fundamental period of the building are taken to vary about the value of the standard spectrum anchored to the PGA-value with a coefficient of variation equal to 0.25.

FRAGILITY CURVES FOR RC BUILDINGS

Figure 2 presents the fragility curves for the frame buildings with open ground storey, designed with the "low- and "medium-level" seismic codes. The vertical dotted line corresponds to the design value PGA = 0.16g prescribed by the current seismic code for new structures in Thessaloniki. Low- and mid-rise buildings are expected to suffer minor damage for low values of PGA, in the order of 0.10g, whereas high-rise buildings are likely to exceed the yielding limit state for PGA higher than 0.30g. Pilotis buildings designed with the 1959 code are likely to reach the ultimate limit state for PGA ≥ 0.30g. Those designed with the 1984 code have substantially better behaviour at this limit state, as evidenced by the higher mean values of the fragility curves, $\mu \geq 0.5$g. In all examined buildings, the ultimate damage state is reached after shear failure of the ground storey columns. Note the significantly larger margin between the two damage states for the buildings designed with the "medium-level" code, compared to their "low-level" code counterparts. This may be attributed to the different spacing of column stirrups, i.e. 200 mm and 100 mm for the buildings designed with the 1959 and the 1984 codes respectively.

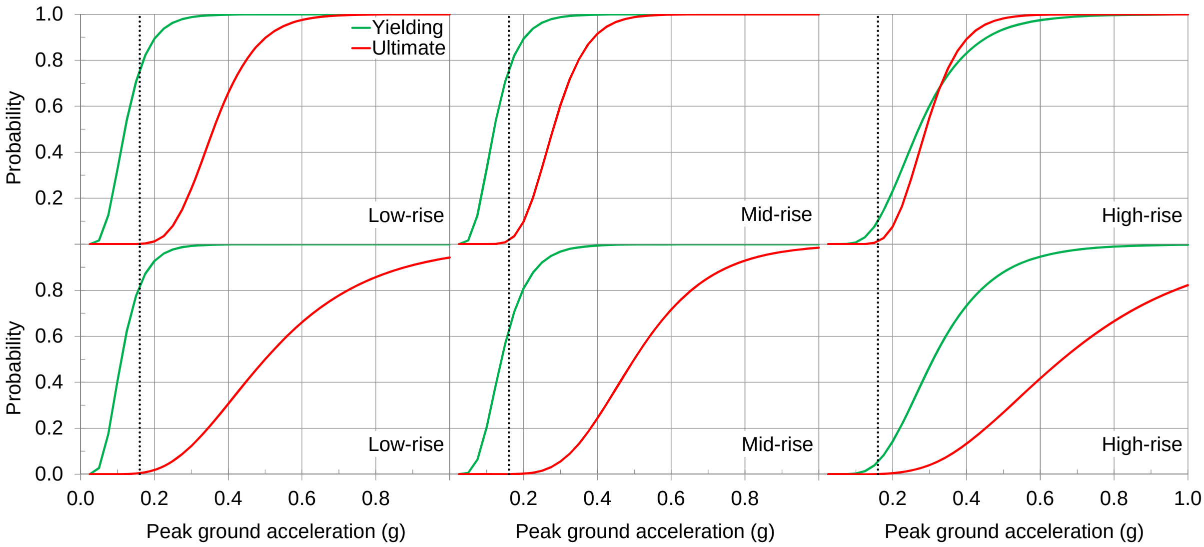

Figure 2. Fragility curves for frame buildings with open ground storey designed with the 1959 (top) and 1984 (bottom) seismic codes

The fragility curves for the infilled frame buildings are shown in Figure 3. They indicate a better behaviour as concerns both damage states in comparison to the buildings with open ground storey. The mean values of the fragility curves for the yielding damage state vary between 0.23g and 0.41g. They are higher for taller buildings and remain practically unchanged for the two levels of seismic design. The ultimate damage state is again due to shear failure of the columns at the ground storey, but it corresponds to higher PGA-values. The mean values of the fragility curves for the buildings with infills in all storeys and designed with the "low- and "medium-level" code are $\mu \geq 0.36$g and $\mu \geq 0.90$, compared to $\mu \geq 0.30$g and $\mu \geq 0.50$ for their counterparts with open ground storey. Note high-rise buildings designed with both the 1959 code (top-right plots in Figures 2 and 3), where the ground storey columns are expected to fail in shear immediately after yielding, or even slightly before.

Lastly, Figure 4 presents the fragility curves for the dual buildings designed with all three seismic codes. In all cases the walls are the critical elements for either damage state. For yielding in particular, the median values of the fragility curves increase marginally with the building height and also for higher-level seismic codes. On the other hand, better seismic design has a marked favourable effect on the probability of exceeding the ultimate damage state. Also for dual buildings, the ultimate damage state is dictated in all cases by the shear failure of the walls at their base.

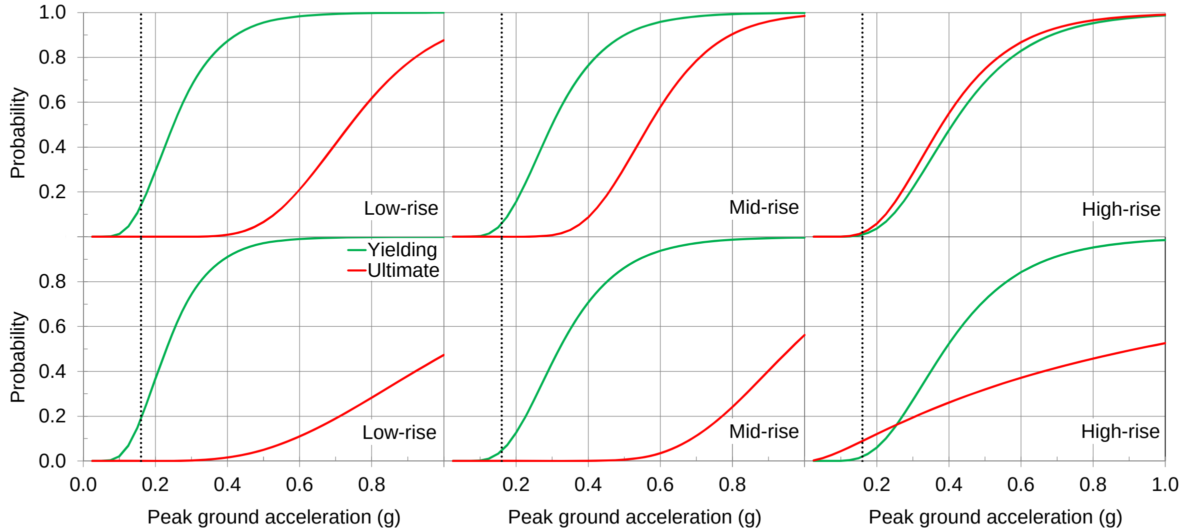

Figure 3. Fragility curves for infilled frame buildings designed with the 1959 (top) and 1984 (bottom) seismic codes

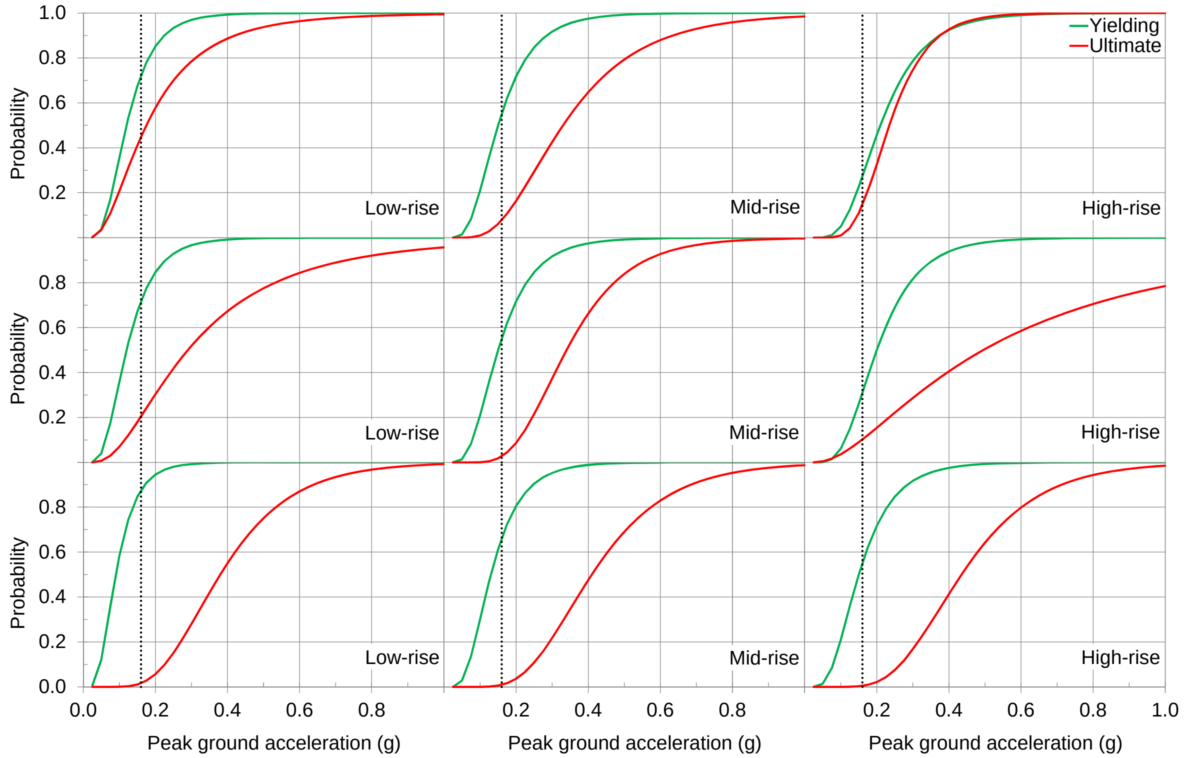

Figure 4. Fragility curves for dual buildings designed with the 1959 (top), 1984 (middle) seismic codes and EC8 (bottom)

For the same level of seismic design and building height, dual systems appear to be more vulnerable than frame structures, even those with open ground storey. Recall, though, that the ultimate damage state corresponds to the exceedance of the shear capacity at a single location of an element and therefore it is not sufficient to describe the overall performance of an individual building for purposes beyond the risk assessment of the building stock at regional level.

Mid-rise dual buildings designed with the 1959 code are the most numerous in the study area. They are expected to show some damage for relatively low values of PGA and substantial damage at moderate levels of PGA (μ = 0.15g and μ = 0.33g respectively for the yielding and ultimate limit states). Yielding is likely to occur at PGA-values close to the design value for new buildings, 0.16g.

FRAGILITY CURVES FOR RC BRIDGES

Figure 5 to 8 present selected results for bridges. Fragility results are presented for the two damage states separately for each pier in the longitudinal (L) and transverse (T) directions and for the whole bridge. The fragility curves for the ultimate state of piers are the envelopes of the curves for flexural and shear failure of the piers. The piers are numbered from the mid-length of the deck to the abutments. The fragility curves for each bridge, shown in the last column of Figures 5 to 8, are those corresponding to a lognormal distribution. The design value of PGA for new bridges in Thessaloniki, according to the current seismic code, is indicated by a vertical dotted line.

Figure 5 presents the fragility curves for two bridges with monolithic connection between the deck and the piers (B04 and B19). Both bridges were constructed after 2000 and have very low probabilities of exceeding the ultimate damage state, even for very high values of PGA. Note the almost identical response of the piers of bridge B19 (with free transverse translation of the deck at the ends) in the two directions. The same holds for the longitudinal direction of bridge B04, whereas different demands are induced in the transverse direction of the piers, because of the restraint of the deck at the abutments.

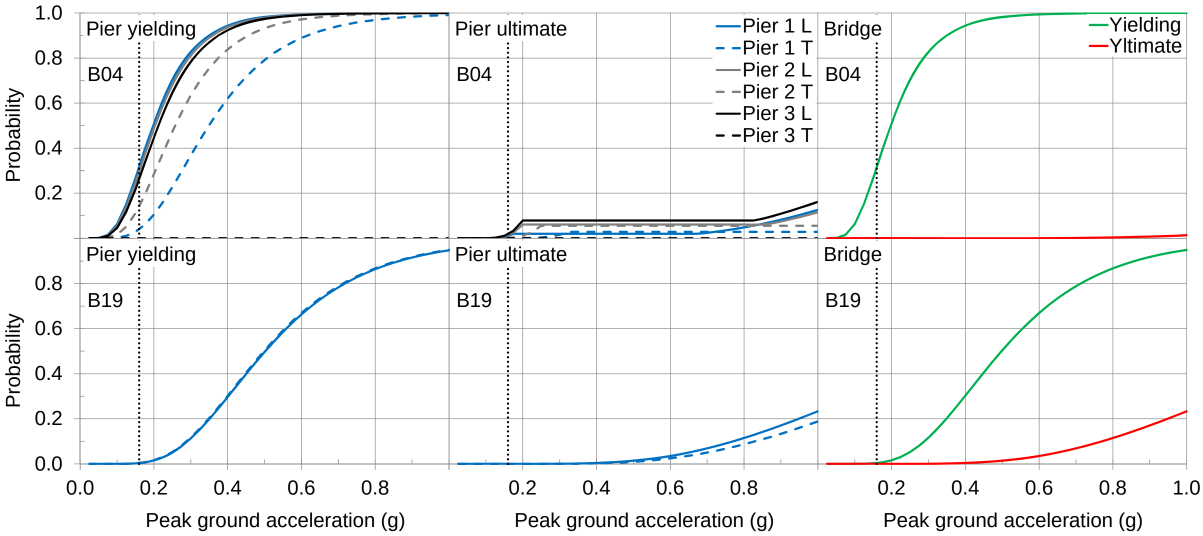

Figure 5. Fragility curves for bridges with continuous deck monolithically connected to the piers: four-span bridge on three-column piers with restrained transverse translation at the abutments (top) and three-span bridge on wall-type piers with free transverse translation at the abutments (bottom)

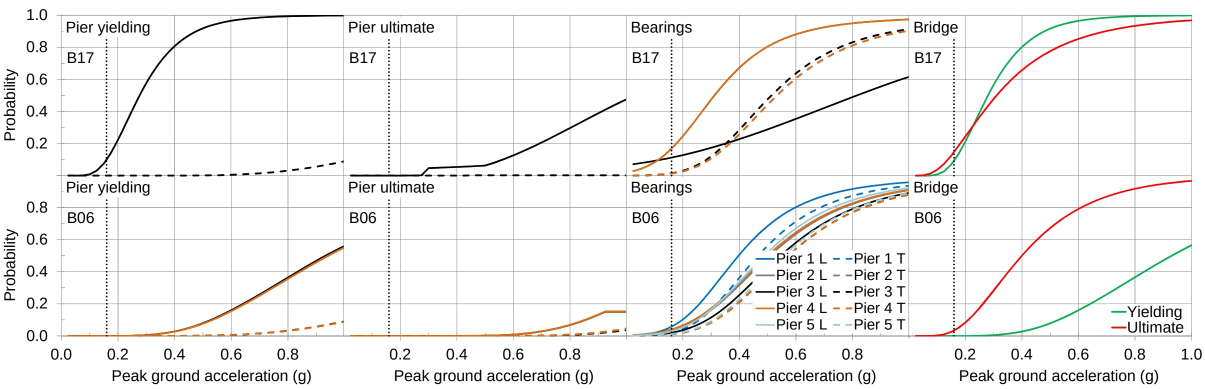

Figure 6. Fragility curves for bridges with continuous deck supported on bearings, wall-type piers and free transverse translation at the abutments: three-span bridge constructed in 1992 (top) and four-span bridge constructed in 2002 (bottom)

Fragility curves for bridges with continuous deck supported on bearings are shown in Figure 6. Different curves are presented for the longitudinal and transverse direction of bearings located on top of each pier; they are the envelopes of the curves corresponding to rollover or shearing. As in all examined bridges of this type, the bearings are critical for the ultimate damage state. It is likely that failure of bearings occurs before yielding of the piers, as is the case for bridge B06 (Figure 6 bottom). The relevant probability, though, is negligible at the level of the design PGA. The comparison of the curves at component and system level shows that bridges designed with "high-level" code (Figure 6 bottom) are expected to suffer less damage than those designed with a "medium-level" code (Figure 6 top). Such difference is more evident on the piers and less so on the bearings.

There are a few bridges in the study area with the deck connected monolithically to the central piers and supported on bearings on top of the others. B07 has five symmetric spans and B15 has seven slightly asymmetric spans. They were both constructed after 2002. Their main difference lies on the height of piers: 6.2 m for B07 and 11.4 m for B15. As shown in Figure 7, the bridge with taller piers is less vulnerable than the one with shorter piers, particularly for the ultimate damage state. Although they belong to the same structural type and were designed with the same code, differences in the base geometry (pier height and number of spans) result in different probabilities of damage. Furthermore, the taller piers result in the shift from shear-dominated failure in B07 to a flexural one in B15.

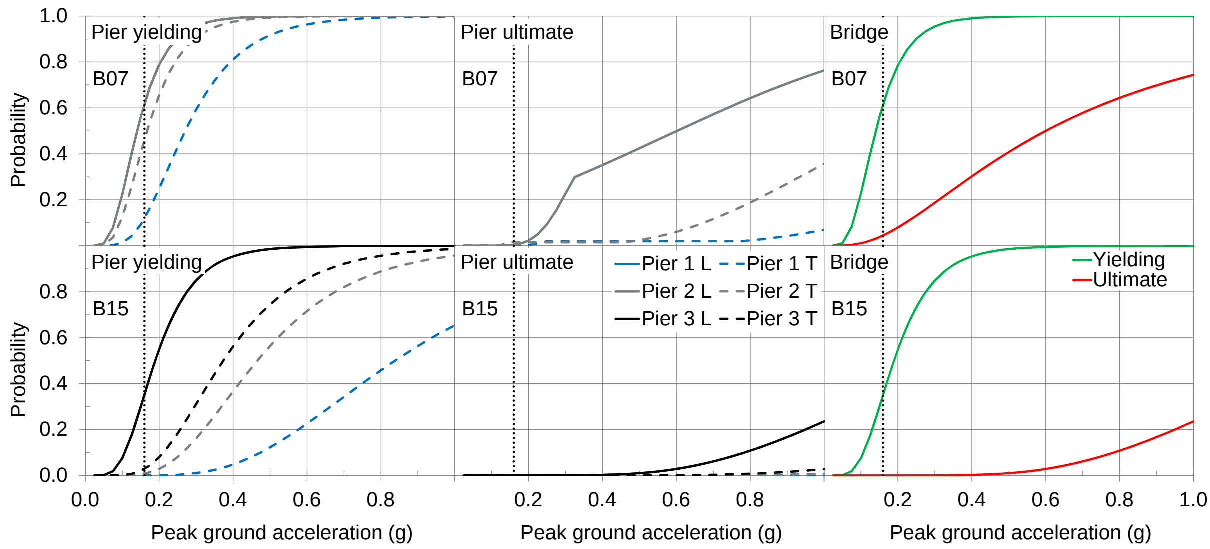

Figure 7. Fragility curves for bridges with continuous deck supported on bearings and monolithic connection at the central piers: five-span (top) and seven-span bridge (bottom)

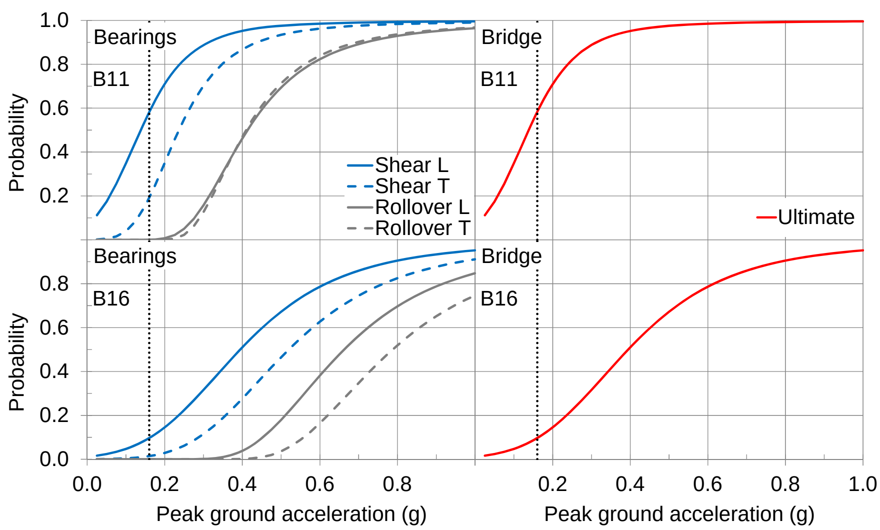

Figure 8. Fragility curves for single-span bridges supported on bearings: 20m-long bridge constructed in 1985 (top) and 21m-long bridge constructed in 1992 (bottom)

Results for single-span bridges are given in Figure 8. Fragility curves are presented for the two possible failure modes of the bearings and for the earthquake action along the two main horizontal directions. Although the two bridges have practically the same length and are presumably designed with the same seismic code, the probabilities of damage at a given PGA-value are significantly different. This observation holds true also for the other four bridges of this type. Further to the different local soil conditions, the decks of the two bridges are of different type and width, and are supported on bearings of different size and number (solid slab on 10 bearings for B11 and precast girders on 18 bearings for B16).

CONCLUSIONS

A methodology for real-time fragility analysis has been applied on the inventory of RC buildings and bridges in Thessaloniki. It performs nonlinear analysis of simplified models of prototype or existing structures, using as input their geometry and reinforcement, and produces seismic fragility curves that account for the uncertainty in the models and the variability of the materials and geometry.

Most buildings in the study area are likely to suffer minor damage (yielding of vertical elements) for peak ground acceleration in the vicinity of the design value stipulated in the current seismic code for new structures. Significant damage (exceedance of the shear capacity of horizontal and/or vertical elements) is expected at twice that value, or above.

The probability of damage on bridges at the design value of PGA is relatively low for most of the examined structures, particularly for those designed with a “high-level” code. However, it is expected that, for PGA close to the design value, the bearings will fail before yielding of the piers in bridges designed with “low- or “medium-level” seismic code.

The obtained results confirm that buildings and bridges designed with modern seismic codes have smaller probability of damage compared to those designed with “low- and “medium-level” codes.

An important remark is that the fragility curves of bridges belonging to a given structural type vary significantly with their basic geometry. Then caution is needed when the most appropriate fragility curves for a bridge are selected among those produced in previous studies. It might be advisable to develop new fragility curves specifically for an individual structure.

The fragility curves presented in this paper were used for the validation study in the city of Thessaloniki (Pitilakis et al., 2014b). In addition to the development of maps showing the distribution of damage for a number of seismic events, they were employed in connectivity analysis of the buildings and the road network (blocked roads due to collapsed buildings) which demonstrated that the estimated losses are much higher when the interaction between systems is considered. The expected damage of buildings was also combined with the projected utility loss of the electric power and water supply networks to estimate the socio-economic consequences of each event in terms of shelter needs.

ACKNOWLEDGMENTS

The research leading to these results received funding from the European Community’s 7th Framework Programme (FP7/2007-2013) under grant agreement n^{o} 244061.

REFERENCES

Antoniou K, Tsionis G, Fardis MN (2014) “Seismic fragility of concrete buildings”, *Proceedings of the Fourth International fib Congress*, Mumbai, India, 10-14 February, paper 62

Bardakis VG and Fardis MN (2011) “Nonlinear dynamic v elastic analysis for seismic deformation demands in concrete bridges having deck integral with the piers”, *Bulletin of Earthquake Engineering* 9(2): 519-536

Biskinis DE and Fardis MN (2013) “Stiffness and cyclic deformation capacity of circular RC columns with or without lap-splices and FRP-wrapping”, *Bulletin of Earthquake Engineering* 11(5): 1447-1466

Biskinis DE and Fardis MN (2010a) “Deformations at flexural yielding of members with continuous or lap-spliced bars”, *Structural Concrete* 11(3): 127-138

Biskinis DE and Fardis MN (2010b) "Flexure-controlled ultimate deformations of members with continuous or lap-spliced bars", *Structural Concrete* 11(2): 93-108

Biskinis DE, Roupakias G, Fardis MN (2004) "Degradation of shear strength of RC members with inelastic cyclic displacements", *ACI Structural Journal* 101(6): 773-783

CEN (2005a) EN 1337-3 Structural bearings - Part 3: Elastomeric bearings, European Committee for Standardization, Brussels

CEN (2005b) EN 1998-2 Eurocode 8: Design of structures for earthquake resistance - Part 2: bridges, European Committee for Standardization, Brussels

CEN (2005c) EN 1998-3 Eurocode 8: Design of structures for earthquake resistance - Part 3: Assessment and retrofitting of buildings, European Committee of Standardization, Brussels

CEN (2004) EN 1998-1 Eurocode 8: Design of structures for earthquake resistance - Part 1: General rules, seismic actions and rules for buildings, European Committee for Standardization, Brussels

CEN (2003) EN 1991-2 Eurocode 1: Actions on structures - Part 2: Traffic loads on bridges, European Committee for Standardization, Brussels

Fardis MN and Tsionis G (2013) "Eigenvalues and modes of distributed-mass symmetric multispan bridges with restrained ends for seismic response analysis" *Engineering Structures* 51: 141-149

Fardis MN, Papailia A, Tsionis A (2012) "Seismic fragility of RC framed and wall-frame buildings designed to the EN-Eurocodes", *Bulletin of Earthquake Engineering* 10(6): 1767-1793

Kappos AJ, Panagiotopoulos C, Panagopoulos G, Papadopoulos E. WP4 – Reinforced Concrete buildings (Level I and II analysis), RISK-UE Report, 2003

Keintzel E (1990) "Seismic design shear forces in RC cantilever shear wall structures", *European Journal of Earthquake Engineering* 3: 7-16

Kosmopoulos A and Fardis MN (2007) "Estimation of inelastic seismic deformations in asymmetric multistory RC buildings", *Earthquake Engineering & Structural Dynamics* 36(9): 1209-1234

Panagiotakos TB and Fardis MN (2004) "Seismic performance of RC frames designed to Eurocode 8 or to the Greek codes 2000", *Bulletin of Earthquake Engineering* 2(2): 221-259

Pitilakis K, Franchin P, Khazai B and Wenzel H (2014) SYNER-G: systemic seismic vulnerability and risk assessment of complex urban, utility, lifeline systems and critical facilities, Springer, Heidelberg

Pitilakis K, Riga E and Anastasiadis A (2012) "Design spectra and amplification factors for Eurocode 8", *Bulletin of Earthquake Engineering* 10(5): 1377-1400